Design and Development of Extremely Low-Frequency Pulsed Electro-magnetotherapy Chamber for In Vivo and In Vitro Studies

Chandra Kant Singh Tekam[1], Ajay Kumar Sahi[1], Saksha Shinde[2], Pooja Kumari[1], Sanjeev Kumar Mahto[1]*

[1]Tissue engineering and Biomicrofluidics Laboratory, School of Biomedical Engineering, Indian Institute of Technology (Banaras Hindu University), Varanasi, India

[2]Department of Biomedical Engineering, Shri Govindram Seksaria Institute of Technology and Science, Indore, India

Corresponding author: Dr. Sanjeev Kumar Mahto

Email: skmahto.bme@iitbhu.ac.in

Address: Tissue Engineering and Biomicrofluidics Laboratory, School of Biomedical Engineering, Indian Institute of Technology (Banaras Hindu University) Varanasi, India

doi: 10.48047/ecb/2023.12.si4.858

Abstract

The application of consistent, highly low-frequency pulsed magnetic fields by a specialized coil system is necessary for bioelectromagnetic applications. This paper presents a detailed discussion of a mono-axial circular Helmholtz coil's design, construction, and set up to generate and maintain a homogenous magnetic field using static/alternating current. The custom-made device was fabricated to achieve cost-effectiveness and less complexity than similar commercial systems. The monoaxial Helmholtz coil can generate a magnetic field ($1\ mT \leq B \leq 3\ mT$) while maintaining field homogeneity ($\geq 90\%$) around the center of coils in each axis. This paper highlights the two main design aspects: first, there is a correlation between wire gauge, coil resistance, coil current, and wire resistance; second, there is the magnetic field validation regarding the homogeneity around the coil's center.

Keywords: Extremely low-frequency (ELF), Pulsed electromagnetic field (PEMF), Static magnetic field (SMF), Standard wire gauge (SWG)

1. Introduction

Bioelectromagnetics is a non-invasive technique providing an alternative therapeutic method for numerous applications. It uses extremely low-frequency magnetic fields (ELF-MFs) for soft and hard tissue treatment. The Helmholtz, Merritt, and Ruben coil arrangements are the most popular design configurations for uniform magnetic field generation systems [1]. However, various bioelectromagnetic studies indicated that the Helmholtz configuration is the most straightforward to implement [2]–[5]. Although the Helmholtz coil's underlying theory is reasonably well

understood, but designing and fabricating a monoaxial coil is not simple and largely depends upon the intended applications. Furthermore, magnetic field strength and uniformity within a given volume, response time, and the coil's inductance can vary significantly depending on the applications.

The design, implementation, and validation of a homogenous alternating magnetic field are represented in this paper. Its primary applications are observing magnetic field exposure effects under *in vivo* and *in vitro* conditions. The materials and methods sections discuss the proposed systems' requirements. The objective is to design and fabricate a PEMF device capable of generating a uniform magnetic field in host cells and tissues.

2. Material and methods

2.1 Design considerations

We selected a circular coil configuration rather than a square one due to its simplicity in design, fabrication, assembly, and cost-effectiveness [6]. The magnetic field must be homogenous with negligible variation, regardless of location within the limited volume. Moreover, the magnetic field must accommodate the animal cage and incubator chamber to confirm adequate exposure under *in vivo* and *in vitro* conditions.

2.2 Mathematical modeling

In custom-made device, it is necessary to determine the magnetic field close to the coil's center. According to the Biot-savart law, the magnetic field depends on the current, number of turns, size, and ideal spacing between coil pairs [7]–[9]. The biot-savart law can be expressed as

$$dB = \frac{\mu_0}{4\pi}\left(\frac{Idl\sin(\theta)}{r^2}\right) \qquad (1)$$

Here,

$I = Current\ flow\ insid$

$dl = Conductor\ element$

$r = Radial\ distance\ between\ dl\ and\ point\ P$

Now as shown in the figure 1(A),

$$dB = \frac{\mu_0 I}{4\pi}\left(\frac{cos\Phi}{d}\right)d\Phi \qquad (2)$$

Hence, the magnetic field due to the whole conductor

$$B = \int dB \qquad (3)$$

$$B = \frac{\mu_0}{2\pi}\left(\frac{I}{d}\right) \qquad (4)$$

Equation (4) gives the value of magnetic flux density (B) at point (P) due to the conductor of infinite length, and for an infinitely long conductor, $\alpha = \beta = \frac{\pi}{2}$ as shown in figure 1(B).

The magnetic field at the center of coaxial coil can be represented by integrating equation (1)

$$B = \frac{\mu_0 I}{4\pi r^2} \int_0^{2\pi r} dl \qquad (5)$$

since θ=90˚

$$B = \frac{\mu_0 NI}{2r} \qquad (6)$$

2.3 Helmholtz coil equation

The Helmholtz coils are widely used for experimental purposes where magnetic field uniformity is crucial, and equation (7) explains the exact value of the magnetic field at the center point [9], [10]**.** The magnetic flux density (*B*)at the midpoint between the coils can be expressed by the following expression

$$B = \left(\frac{4}{5}\right)^{3/2} \left(\frac{I*N*\mu}{R_c}\right) \qquad (7)$$

Here,

$B = magnetic\ flux\ density$

$N = number\ of\ wire\ turns$

$R_c = coil\ radius$

$I = current\ through\ coils$

and

$\mu = permiability\ of\ space (4\pi \text{ x } 10^{-7} \text{T m/A})$

The Helmholtz coil configuration and magnetic field orientation of the PEMF exposure system is depicted in figures (2A & 2B).

2.4 Optimum distance between coils

According to the Helmholtz configuration, co-axial circular coils must be arranged symmetrically, one on each side of the experimental area separated by a distance ($r = 0.265\ m$) equal to the coils radius as shown in the following expression

$$r = R_c \qquad (8)$$

Each coil must carry an equal amount of current in the same direction to reduce the non-uniformity of the field at the coils' centers and magnetic flux density (B) gets affected by increasing the coil separation distance (r) [11]–[13].

2.5 Helmholtz coil configuration

The magnetic flux density shown by equation (7) is proportional wire turns (N), and supplied current (I) but inversely proportional to the coil radius (R_c). Therefore, any changes in the structural dimensions will be implicated in selecting structural and electrical aspects like the number of wires turn, wire length, and uniformity within the cubic sections.

2.5.1 Structural design

The monoaxial coil system should generate homogenous magnetic field, considering the requirement of a $30 \times 35.5\ cm^2$ the region with minimum field variation, as illustrated in figure 2(A). Figure 2(B) illustrates the magnetic field direction due to the current flow inside coils.

2.5.2 Electrical design

The primary considerations in designing an effective Helmholtz coil system are reducing coil impedance and maintaining spatial limitations, field gradient, and field intensity between the coils. In addition, several other factors, i.e., wire gauge, no. of wire turns, and coil circuit configuration, must be considered [14]–[17] as shown in figure 3.

2.5.2.1 Spatial limitations

According to Helmholtz coil configuration, we need to maintain the coil separation distance (r) equal to the coil radius (R_c) as shown in equation (7). Here, the coil separation distance is equivalent to "$(d_w \times N^{0.5})$" for a square cross-section with no. of turns (N), wire diameter (d_w) and thickness of coil [18]. Then, we must consider the following expression

$$d_w) \times N^{\frac{1}{2}} < \frac{D}{2} \qquad (9) \qquad (9)$$

Here,

$D = Coil\ diameter\ in\ meters$

Now, the total wire resistance can be represented by the following expression

$$R = \rho(\frac{L_w}{A}) \qquad (10)$$

and

$$L_w = \frac{R\pi {d_w}^2}{4\rho} \qquad (11)$$

Here,

$R = Resistance\ of\ straight\ wire\ in\ ohm\ (\Omega)$
$d_w = Diameter\ of\ wire\ in\ meters$
$D = Coil\ diameter\ in\ meters$
$L_w = Length\ of\ wire\ in\ meters$
$\rho = Resistivity\ of\ wire$

$$l = 2\pi\frac{D}{2}N \qquad (12)$$

Therefore,

$$N = \frac{R(d_w)^2}{4\rho D} \qquad (13)$$

as d_w increases,$t = d_w \times N^{0.5}$, using equation (13), gives

$$t = (d_w)^2(\frac{R}{4\rho D})^{\frac{1}{2}} \qquad (14)$$

the influence of spatial limitations and relationship between magnetic flux density (B), wire radius, and cross-sectional area of wire is depicted in figure (4 &5).

2.5.2.2 Coil inductance

The following expressions can calculate the self-inductance and loop inductance of the conductor:

$$L_{wire} = 2L_w\left[ln\left\{(\frac{2L_w}{d_w})\left(1+\sqrt{1+(\frac{d_w}{2L_w})^2}\right)\right\} - \sqrt{1+\left(\frac{d_w}{2L_w}\right)^2} + \frac{\mu}{4} + \left(\frac{d_w}{2L_w}\right)\right] \qquad (15)$$

and

$$L_{loop} = \mu_0\mu_r(\frac{D}{2})[\ln\left(\frac{8D}{d_w}\right) - 2] \qquad (16)$$

Here,

$L_{wire} = Inductance\ of\ straight\ wire\ in\ henries\ (H)$

$d_w = Diameter\ of\ wire\ in\ meters$

$L_w = Length\ of\ wire\ in\ meters$

$D = Coil\ diameter\ in\ meters$

$\mu = Permiability$

$\mu_0 = Permiability\ of\ free\ space\ (4\pi \times 10^{-7})$

$\mu_r = Relative\ permiability$

In Helmholtz coil configuration, the coil inductance, mutual inductance, and coupling factor can be represented by the following expressions

$$L_{coil} = \mu_0\mu_r\frac{A*N^2}{2*R_c} \qquad (17)$$

and

$$M = \sqrt{L_{coil1} * L_{coil2}} \qquad (18)$$

and

$$K = \frac{M}{\sqrt{L_{coil1}*L_{coil2}}} \qquad (19)$$

Here,

$L_{coil} = Inductance\ of\ coil\ in\ henries\ H$

$M = Mutual\ inductance\ of\ coil\ in\ henries\ H$

$k = Coupling\ factor\ between\ coil$

In the Helmholtz coil system, the connection can be a series or parallel circuit depending upon the requirement, i.e., static/pulsed magnetic field.The power supply frequency is extremely low-frequency (≈ 50 Hz) under experimental conditions. Hence, the Helmholtz coil shown here is better suited for ELF applications [19]–[21].

The apparent power is the total power available to run any device, butthe real power is used for a specific load.Apparent power is a combination of real power and reactive power. Real power is a result of resistive components, and reactive power is a result of capacitive and inductive components; these components are commonly implemented in all circuits. The apparent power (s), real power (P), and reactive power (Q) is represented by the following expressions

$$S = V * I * e^{j\theta} \quad (20)$$

and

$$S = V * I * \{\cos(\theta) + jsin(\theta)\} \quad (21)$$

As shown in equations (20) & (21), real power (P) and reactive power (Q) can be expressed as

$$P = VI\cos(\theta) \quad (22)$$

and

$$Q = VI\,jsin(\theta) \quad (23)$$

Here,

$V = Voltage\ in\ the\ circuit$

$I = Current\ in\ the\ circuit$

$\theta = Angle\ between\ voltage\ and\ current\ in\ the\ circuit$

The Helmholtz coil system's electrical design depends on selectinga wire gauge to facilitate ease in the coiling process, limit the wire length and the number of wire turns to control the coil's total inductance[22] as depicted in figure 5. Hence, we selected 20 standard wire gauges (SWG) to support current levels ($\leq 4\ A$) without overheating or losing the insulation capacity of wires. As mentioned in equation (7), (12), and (13), magnetic flux density (B),the wire turns (N), total Resistance (R), and length of wire (L_w) is calculated, which is summarized in Table 1. It is crucial to note that the current, voltage, and power are maximum values in current experimental conditions.

Table 1 manifests the design framework concerning the fabrication of the device. The coil inductance and mutual inductance are almost the same according to equations (17) & (18), and the coupling factor is equal to one, as represented in equation (19). Table 2 & 3 represents the electrical parameters obtained on the Helmholtz coil prototype for generating and maintaining the magnetic field.

2.6 Helmholtz coil system

The construction details of Helmholtz coils were similar to the previous studies [23]. The resistance and inductance are almost the same as calculated, indicating the device will operate as expected.

2.7 Current source

The magnetic field generation inside the Helmholtz coil system is accomplished by maintaining the alternating current flow through the conductor coil. A duty cycle is the fraction of one period in which a signal or system is active, and it is percentage or a ratio of the on-and-off cycle [24]. The duty cycle is important because a slight increase/decrease may lead to a significant increase/decrease in the operating peak current and corresponding magnetic fields. The supplied current has a frequency (50 Hz) and duty cycle (50%). The Helmholtz coil requires electrical current ($1\ A < I < 3\ A$) and assuming that the coil has the highest Resistance ($23.3\ \mathrm{fi}/coil$), powering the coil requires less than $600\ watt$ for maximum current ($I \leq 3\ A$). The custom-made Helmholtz coil system and schematic arrangement of the Helmholtz coil setup for bioelectromagnetic studies is shown in figure (6). Figure (7) illustrates the schematic for the arrangement of the power supply followed by variable autotransformer, step-up transformer, and digital ammeter/voltmeter connected with Helmholtz coil (parallel configuration) for generation of homogenous magnetic field for *in vivo* and *in vitro* studies.

3. Results

3.1 Magnetic field analysis

3.1.1 Computational simulation of MF distribution and intensity

The analysis of spatial MF distribution between monoaxial Helmholtz coil systems for outer diameter ($D_1 = 0.530\ m$), inner diameter ($D_2 = 0.490\ m$), coil thickness ($t = 0.020\ m$), and coil separation distance ($r = 0.265\ m$) were analyzed. The current direction in coils is shown in figure 2(B). At the supply current range ($1A < I < 3A$), it was found that magnetic flux density was significantly dependent on the number of wires turn and distance, as shown in figures 8(A, B & C). Magnetic flux direction mainly depends on selecting the current direction in both coils. The field generated from coils becomes additive, and we successfully achieved the uniform MF distribution inside the exposure chamber, as shown in figures 9(A, B & C). In our study, the dimensions of coils were selected for *in vitro* and *in vivo* experiments. Hence, the custom-made device can be used for various applications, i.e., soft/hard tissue at different loading voltages.

3.12 Homogeneity test

The measurement of magnetic flux density was performed with a handheld magnetic field sensor (MG3002, Lutron Electronic, Taiwan) and an acrylic sheet arrangement ($l = 20$ cm $=$ 0.5 cm $= 44.5$ cm.) with equidistant holes that were initially placed on $\mathrm{x} = 0 \quad = 0\ \mathrm{z} = 0$ as mentioned in previous studies [23]. The supply voltage and current were gradually increased up to $V = 75\ volts\ \&\ I = 1\ A$ thus creating a homogenous field around the center as shown in figure (10). The measurements were obtained for the yz-plane at x = 0, and all readings were taken as coordinates at every 2 cm slot mark on the acrylic sheet while keeping $\mathrm{x} = 0, \mathrm{y} = -5$ to 5, and $\mathrm{z} = -7$ to 7 for one set of readings. The above process of homogenous magnetic field generation was also repeated for $V = 120\ \&\ 190\ volts\ \&\ I = 2\ \&\ 3\ A$ respectively as

shown in figures 10(A, B & C). Tables 3 & 4 show the electrical parameters and magnetic field homogeneity data, as represented in figure (5 & 10) respectively. Table 5 shows the temperature variation in coils during the experimental duration.

4. Discussion

The monoaxial Helmholtz coil system accomplished great results compared to other magnetic field generation systems mentioned in the literature. The application of metallic core was reduced using plywood sheets to provide structural stability, easy to be manufactured and assembled quickly at a reasonable cost for our application.

The Helmholtz coil with an outer diameter ($D_1 = 0.530\ m$), inner diameter ($D_2 = 0.490\ m$), coil thickness ($W = 0.020\ m$) at $N = 540$ was constructed using 20 SWG copper stranded wires for maximizing the coil current due to an increase in cross-sectional area and reduction in coil resistance to generate a homogenous magnetic field without increasing the wire length as per equations (7), (12) & (13). The coil system will be mainly used for bio-electromagnetics applications. The device's capability to generate a magnetic field ($\leq 3\ mT$) can cancel the earth's magnetic field ($\leq 1.2\ Gauss$) on any axis. The coils are being supplied by voltage supply ($75 - 190\ volts$), 50 Hz power supply for establishing a magnetic field ($B = 1 - 3\ mT$). No EM wave would emit from coils at this low frequency, and hence there won't be any electromagnetic interference issue. Hence faraday cage is not required in the present setup. The custom-made coils for the experimental setup were multiturn instead of single-turn solid conductor coils to avoid eddy current flows in the coil due to the skin effect and proximity effect. Hence it can be reasonably assumed that working (AC) resistance is more or less equal to apparent (DC) resistance and reasonably accurate results can be anticipated. In the present study, we also performed the temperature variation analysis to determine the temperature at the end of the exposure period. We have designed the incubation chamber with a 0.5 cm thick acrylic sheet having dimensions $length = 30\ cm, height = 17\ cm, width = 25\ cm$ as shown in figures (6) for *in vitro* studies. The incubation chamber was equipped with a temperature sensor and controller (tAPMAN 48 7E-1) and distilled water in a petri-dish to maintain temperature (37 ± 2 ˚C) and humidity inside the chamber. We used a Mextech DT-9 pen-type stainless steel thermometer to observe the temperature variation under standard laboratory conditions, as illustrated in Table 5.

Moreover, the results show that magnetic field is homogenous around the incubation chamber at the coil's center, as shown in figure 10. Another advantage of the system is the current required to generate a homogenous magnetic field inside the coils, since the minimum and maximum value of current ($I = 1 - 3\ A$) and considering each pair resistance, power ($P \leq 600\ watt$) is required to power the coils for different voltage ranges as shown in Table-1. Table 2 & 3 show the obtained electrical parameters and magnetic field homogeneity data for the total area ($30 \times 35.5\ cm^2$): the field strength at the center, the highest and lowest field strength in the region, respectively.

5. Conclusion

In this paper, we have discussed the significant design factors, i.e., wire gauge and spatial limitations, involved in the design of Helmholtz coil system for *in vivo* or *in vitro* bioelectromagnetic studies as reported by various research articles [25]–[27]. We have inscribed all significant factors in design and development along with mathematical expressions of the geometric parameters. The Helmholtz coil configuration was employed to improve the quality of the magnetic field uniformity and reduce the losses [15] at the applied frequency.

The main benefit of the current setup was minimal interference from ferromagnetic materials on the Helmholtz coil environment. Despite using a more straightforward constructive design, the results were better than other coils described in the literature.

Author contributions

Conceptualization, Methodology, Software: Chandra Kant Singh Tekam, Saksha Shinde, Sanjeev Kumar Mahto; *Validity tests, Data curation, Writing- Original draft preparation:* Chandra Kant Singh Tekam, Sanjeev Kumar Mahto*; Visualization, Investigation*: Chandra Kant Singh Tekam, Saksha Shinde; *Supervision*: Sanjeev Kumar Mahto; *Software, Validation*: Chandra Kant Singh Tekam, Ajay Kumar Sahi, Saksha Shinde, Sanjeev Kumar Mahto; *Writing- Reviewing and Editing*: Chandra Kant Singh Tekam, Ajay Kumar Sahi, Saksha Shinde, Pooja Kumari, Sanjeev Kumar Mahto;

Acknowledgments

The authors would like to thank the Ministry of Human Resource Development (MHRD), Government of India, for providing financial support. We, as authors, also want to extend sincere gratitude to Dr. R.K. Shrivastava, Professor, Department of Electrical Engineering, Indian Institute of Technology (BHU) Varanasi, and Aditya Kumar, Postgraduate student at the Department of electrical engineering, Indian Institute of Technology (BHU), Varanasi.

Conflict of Interest Statement

The authors declare no conflict of interest.

References:

[1] A. Modi *et al.*, "Hexagonal coil systems for uniform magnetic field generation," in *2016 IEEE Asia-Pacific Conference on Applied Electromagnetics (APACE)*, IEEE, 2016, pp. 47–51.

[2] B. Rubik, "The biofield hypothesis: Its biophysical basis and role in medicine," *J. Altern. Complement. Med.*, vol. 8, no. 6, pp. 703–717, 2002.

[3] N. M. Shupak, F. S. Prato, and A. W. Thomas, "Therapeutic uses of pulsed magnetic-field exposure: a review," *URSI Radio Sci. Bull.*, vol. 2003, no. 307, pp. 9–32, 2003.

[4] C. K. S. Tekam, A. K. Tripathi, G. Kumar, and R. Patnaik, "Emerging role of electromagnetic field therapy in stroke," in *Advancement in the Pathophysiology of Cerebral Stroke*, Springer, 2019, pp. 93–102.

[5] C. Vallbona and T. Richards, "Evolution of magnetic therapy from alternative to traditional medicine," *Phys. Med. Rehabil. Clin. N. Am.*, vol. 10, no. 3, pp. 729–754, 1999.

[6] H. Kohli *et al.*, "Design and study of novel tunable ELF-PEMF system for therapeutic applications," *IETE J. Res.*, vol. 68, no. 4, pp. 2723–2735, 2022.

[7] E. C. Caparelli and D. Tomasi, "An Analytical Calculation of the Magnetic Field Using the Biot Savart Law," *Rev. Bras. Ensino Física*, vol. 23, no. 3, 2001, doi: 10.1590/s0102-47442001000300005.

[8] A. F. R. Alvarez, E. Franco-Mejia, and C. R. Pinedo-Jaramillo, "Study and analysis of magnetic field homogeneity of square and circular helmholtz coil pairs: A taylor series approximation," in *Proceedings of the 6th Andean Region International Conference, Andescon*, 2012, pp. 77–80. doi: 10.1109/Andescon.2012.27.

[9] A. F. Restrepo-álvarez, E. Franco-Mejía, H. Cadavid-Ramírez, and C. R. Pinedo-Jaramillo, "A simple geomagnetic field compensation system for uniform magnetic field applications," *Rev. Fac. Ing. Univ. Antioquia*, no. 83, pp. 65–71, 2017, doi: 10.17533/udea.redin.n83a09.

[10] A. F. R. Alvarez, E. Franco-Mejia, and C. R. Pinedo-Jaramillo, "Study and analysis of magnetic field homogeneity of square and circular helmholtz coil pairs: A taylor series approximation," *Proc. 6th Andean Reg. Int. Conf. Andescon 2012*, vol. 0, no. 2, pp. 77–80, 2012, doi: 10.1109/Andescon.2012.27.

[11] I. S. Grant and W. R. Phillips, *Electromagnetism*. John Wiley & Sons, 2013.

[12] D. S. Jones, *The theory of electromagnetism*. Elsevier, 2013.

[13] E. Ramsden, *Hall-effect sensors: theory and application*. Elsevier, 2011.

[14] A. Mahnam, H. Yazdanian, and M. Mosayebi Samani, "Comprehensive study of Howland circuit with non-ideal components to design high performance current pumps," *Measurement: Journal of the International Measurement Confederation*, vol. 82. pp. 94– 104, 2016. doi: 10.1016/j.measurement.2015.12.044.

[15] L. Raganella, M. Guelfi, and G. D'Inzeo, "Triaxial exposure system providing static and low-frequency magnetic fields for in vivo and in vitro biological studies," *Bioelectrochem. Bioenerg.*, vol. 35, no. 1–2, pp. 121–126, 1994, doi: 10.1016/0302-4598(94)87022-5.

[16] D. Cvetkovic and I. Cosic, "Modelling and design of extremely low frequency uniform magnetic field exposure apparatus for in vivo bioelectromagnetic studies," in *29th Annual International Conference of the IEEE Engineering in Medicine and Biology Society*, 2007, pp. 1675–1678. doi: 10.1109/IEMBS.2007.4352630.

[17] D. Cvetkovic, E. Jovanov, and I. Cosic, "Alterations in human EEG activity caused by extremely low frequency electromagnetic fields," in *International Conference of the IEEE Engineering in Medicine and Biology - Proceedings*, 2006, pp. 3206–3209. doi:10.1109/IEMBS.2006.259314.

[18] C. Salvatore, L. Antonino, R. F. Francesco, and S. Alessandro, "Accurate design of Helmholtz coils for ELF Bioelectromagnetic interaction by means of Continuous FSO," *Int. J. Appl. Electromagn. Mech.*, vol. 39, no. 1–4, pp. 665–669, 2012, doi: 10.3233/JAE-2012- 1526.

[19] E. L. Bronaugh, "Helmholtz coils for calibration of probes and sensors: limits of magnetic field accuracy and uniformity," in *IEEE International Symposium on Electromagnetic Compatibility*, 1995, pp. 72–76. doi: 10.1109/ISEMC.1995.523521.

[20] E. R. Javor and T. Anderson, "Design of a Helmholtz coil for low frequency magnetic field susceptibility testing," in *IEEE International Symposium on Electromagnetic Compatibility*, IEEE, 1998, pp. 912–917. doi: 10.1109/isemc.1998.750329.

[21] T. Anderson, "Design of a Helmholtz coil for susceptibility testing using variational calculus and experimental verification," *IEEE Int. Symp. Electromagn. Compat.*, vol. 2, no. 3, pp. 601–604, 1999, doi: 10.1109/ISEMC.1999.810084.

[22] D. S. Batista, F. Granziera, M. C. Tosin, and L. F. de Melo, "Three-Axial Helmholtz Coil Design and Validation for Aerospace Applications," *IEEE Trans. Aerosp. Electron. Syst.*, vol. 54, no. 1, pp. 392–403, Feb. 2018, doi: 10.1109/TAES.2017.2760560.

[23] C. K. S. Tekam *et al.*, "Effects of ELF-PEMF exposure on spontaneous alternation, anxiety, motor co-ordination and locomotor activity of adult wistar rats and viability of C6 (Glial) cells in culture," *Toxicology*, vol. 485, p. 153409, Feb. 2023, doi: 10.1016/j.tox.2022.153409.

[24] M. C. Brown, *Practical switching power supply design*. Elsevier, 2012.

[25] R. Lodato, C. Merla, R. Pinto, S. Mancini, V. Lopresto, and G. A. Lovisolo, "Complex magnetic field exposure system for in vitro experiments at intermediate frequencies," *Bioelectromagnetics*, vol. 34, no. 3, pp. 211–219, 2013, doi: 10.1002/bem.21758.

[26] K. Paksy, G. Thuróczy, Z. Forgács, P. Lázár, and I. Gáti, "Influence of sinusoidal 50-Hz magnetic field on cultured human ovarian granulosa cells," *Electromagn. Biol. Med.*, vol. 19, no. 2, pp. 91–97, 2000.

[27] P. A. Valberg, "Designing EMF experiments: What is required to characterize 'exposure'?," *Bioelectromagnetics*, vol. 16, no. 6, pp. 396–401, 1995, doi: 10.1002/bem.2250160608.

Figures:

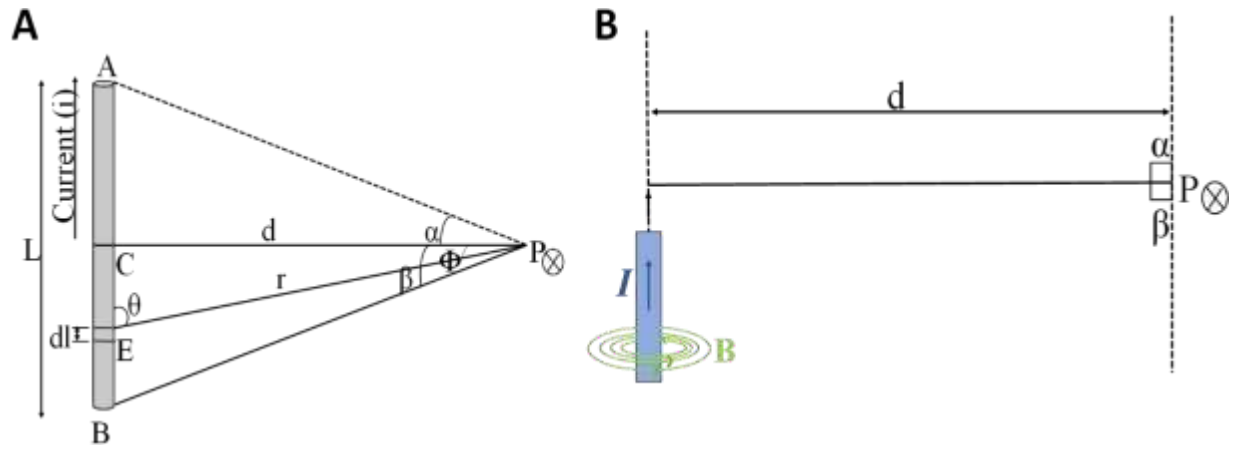

Figure 1. Biot-savart law (A) Magnetic field generation at point "P" along section dl at radial distance r, **(B)** The representation of the magnetic field orientation along wire length.

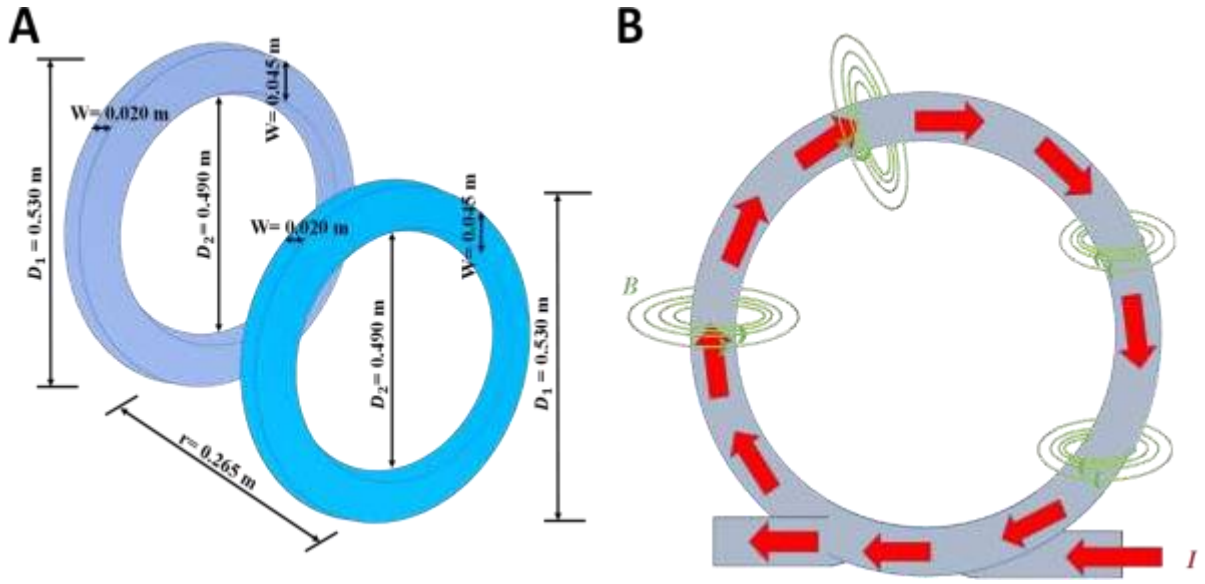

Figure 2. **Structural design of Helmholtz coil system (A)** Schematic of Helmholtz coils, **(B)** Magnetic field orientation due to current flow inside coils. All dimensions are given in meters.

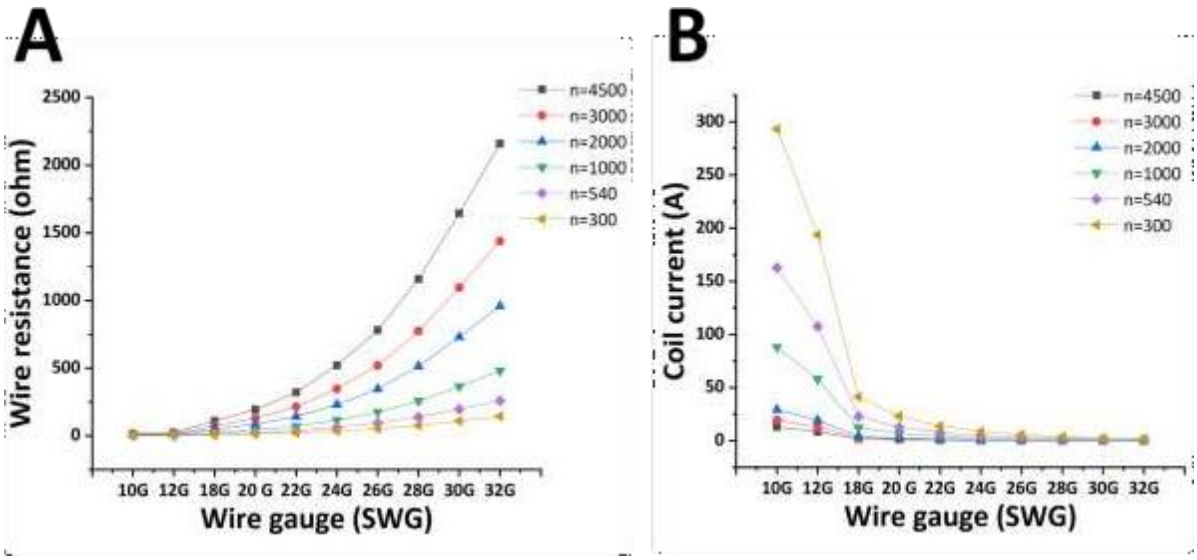

Figure 3. Relationship between wire gauge, coil current, and wire resistance (**A**) Relationship between wire resistance and wire gauge, (**B**) Relationship between coil current and wire gauge

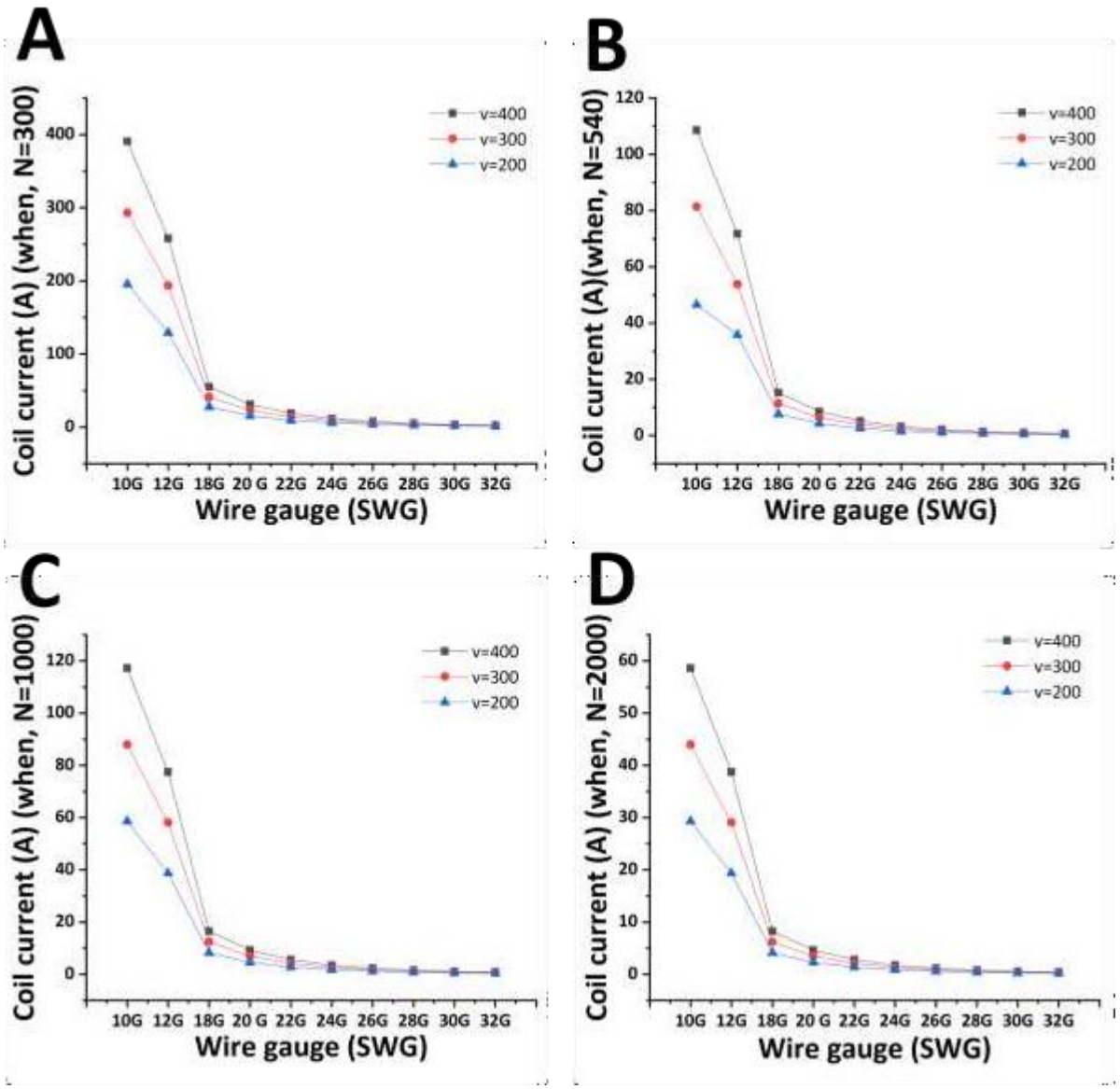

Figure 4. Spatial limitations in the development of Helmholtz coils (**A**) Relationship between coil current and wire gauge when no. of wire turns (N) is 300 turns/coil, (**B**) Relationship between coil current and wire gauge when no. of wire turns (N) is 540 turns/coil, (**C**) Relationship between coil current and wire gauge when no. of wire turns (N) is 1000 turns/coil, (**D**) Relationship between coil current and wire gauge when no. of wire turns (N) is 2000 turns/coil

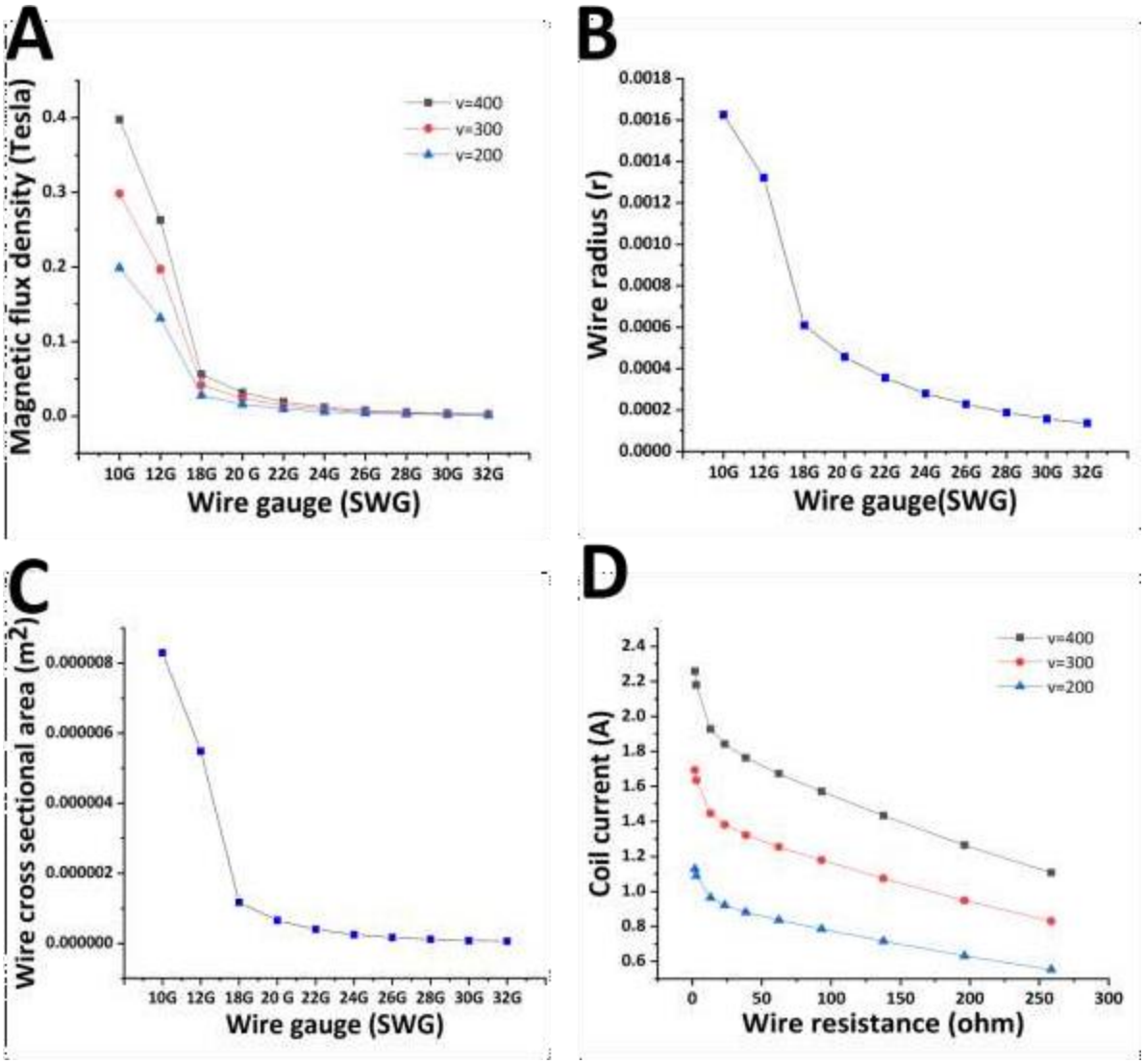

Figure 5. Relationship between magnetic flux density, wire radius, cross-sectional area and wire gauge (**A**) Relationship between magnetic flux density and wire gauge, (**B**) Relationship between wire radius and wire gauge, (**C**) Relationship between cross-sectional area and wire gauge, (**D**) Relationship between coil current and wire resistance.

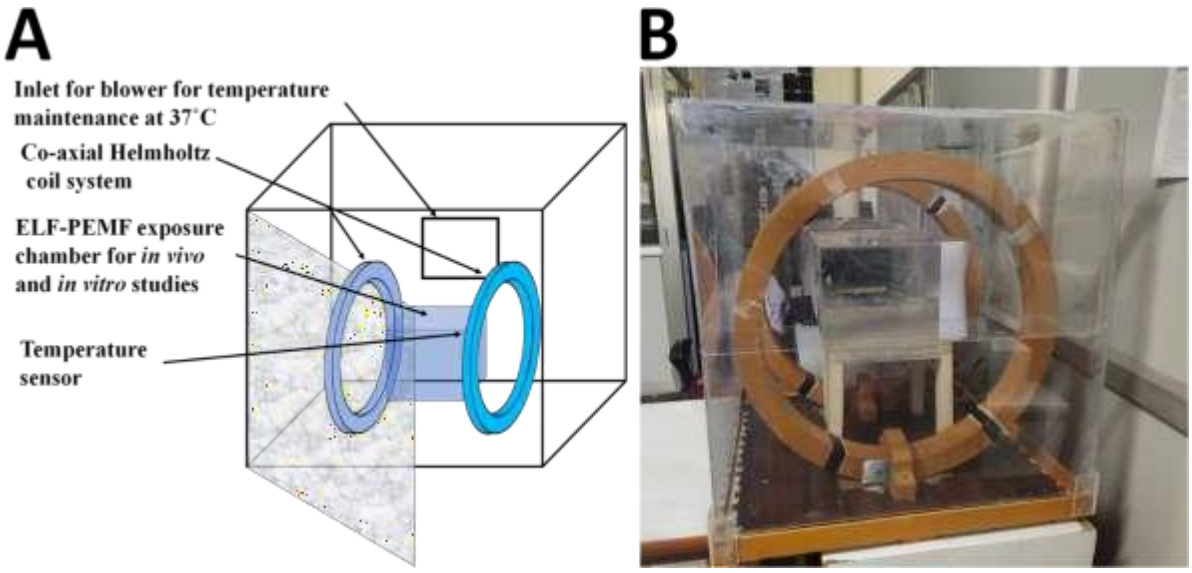

Figure 6. Mono-axial Helmholtz coil (parallel configuration) for in vivo and in vitro studies (**A**) Schematic representation for ELF-PEMF chamber, (**B**) Custom-made ELF-PEMF chamber

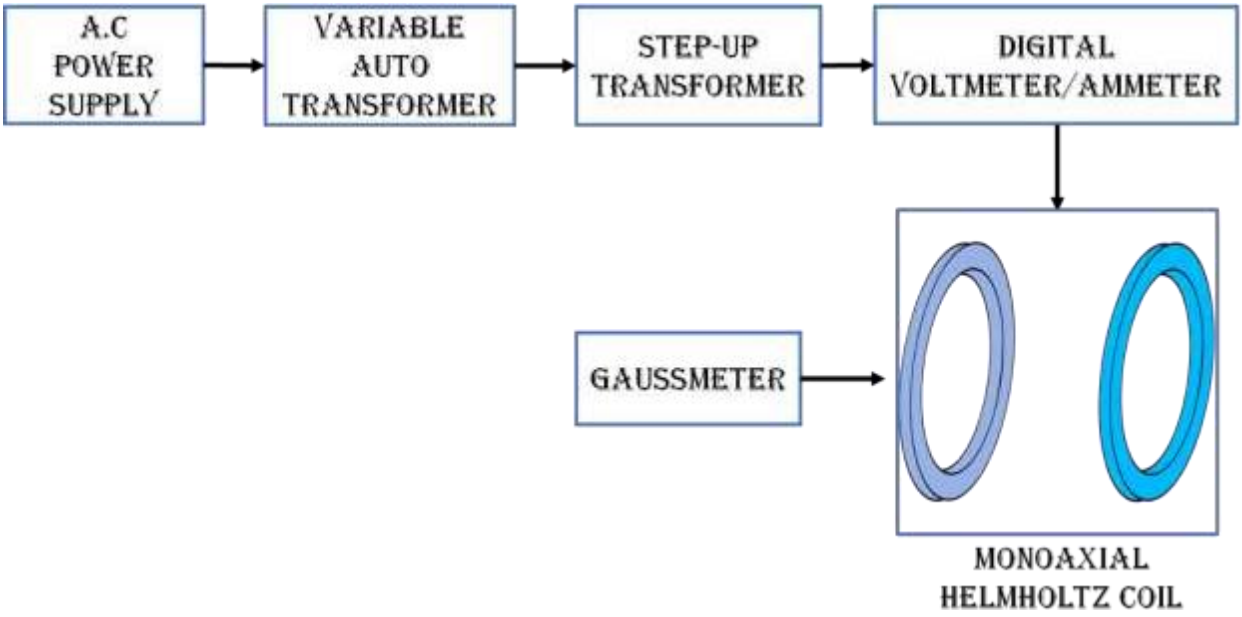

Figure 7. Schematic arrangement of the Helmholtz coil setup Bioelectromagnetic studies

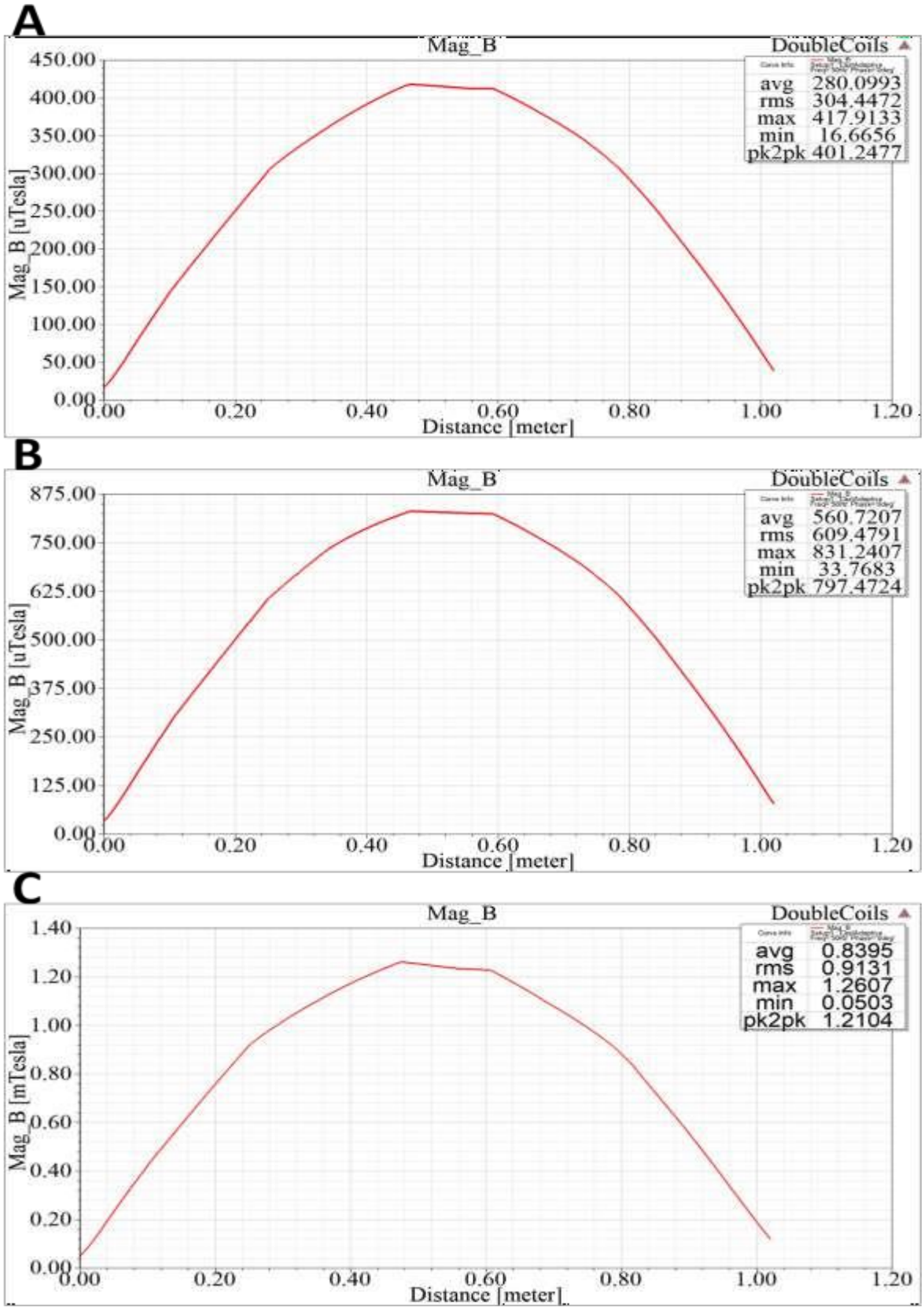
A
Mag_B
DoubleCoils
avg 280.0993
rms 304.4472
max 417.9133
min 16.6656
pk2pk 401.2477
Mag_B [uTesla]
450.00
400.00
350.00
300.00
250.00
200.00
150.00
100.00
50.00
0.00
0.00 0.20 0.40 0.60 0.80 1.00 1.20
Distance [meter]
B
Mag_B
DoubleCoils
avg 560.7207
rms 609.4791
max 831.2407
min 33.7683
pk2pk 797.4724
Mag_B [uTesla]
875.00
750.00
625.00
500.00
375.00
250.00
125.00
0.00
0.00 0.20 0.40 0.60 0.80 1.00 1.20
Distance [meter]
C
Mag_B
DoubleCoils
avg 0.8395
rms 0.9131
max 1.2607
min 0.0503
pk2pk 1.2104
Mag_B [mTesla]
1.40
1.20
1.00
0.80
0.60
0.40
0.20
0.00
0.00 0.20 0.40 0.60 0.80 1.00 1.20
Distance [meter]

Figure 8. Magnetic flux density between Helmholtz coils at different current intensities. (A) Magnetic flux density at y-axis ($I = 1\ A$), **(B)** Magnetic flux density at y-axis ($I = 2\ A$), **(C)** Magnetic flux density at y-axis ($I = 3\ A$).

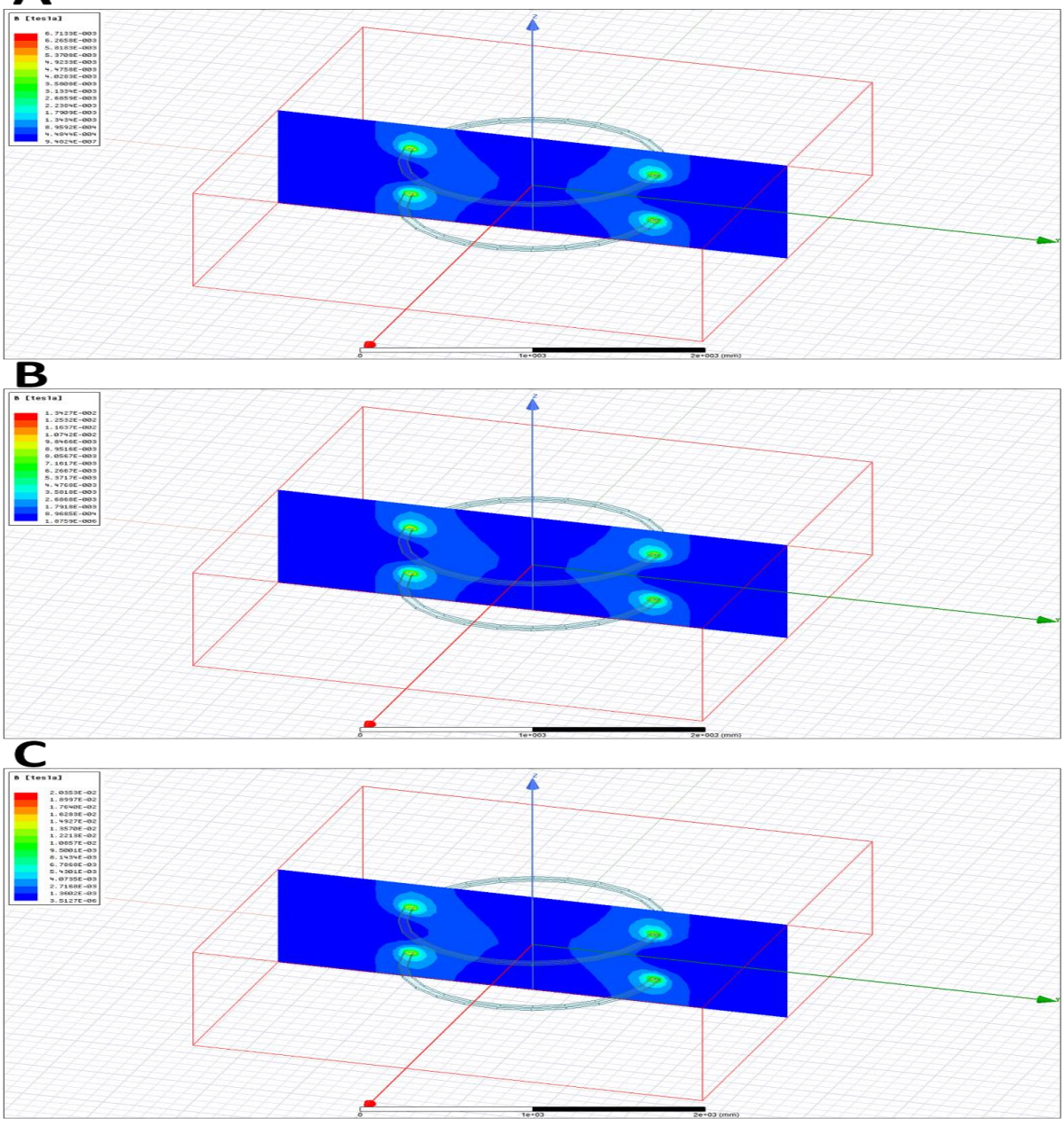

Figure 9. Magnetic field overlay between Helmholtz coils at different current intensities. **(A)** Magnetic field overlay at yz-plane ($I = 1\ A$), **(B)** Magnetic field overlay at yz-plane ($I = 2\ A$), **(C)** Magnetic field overlay at yz-plane ($I = 3\ A$).

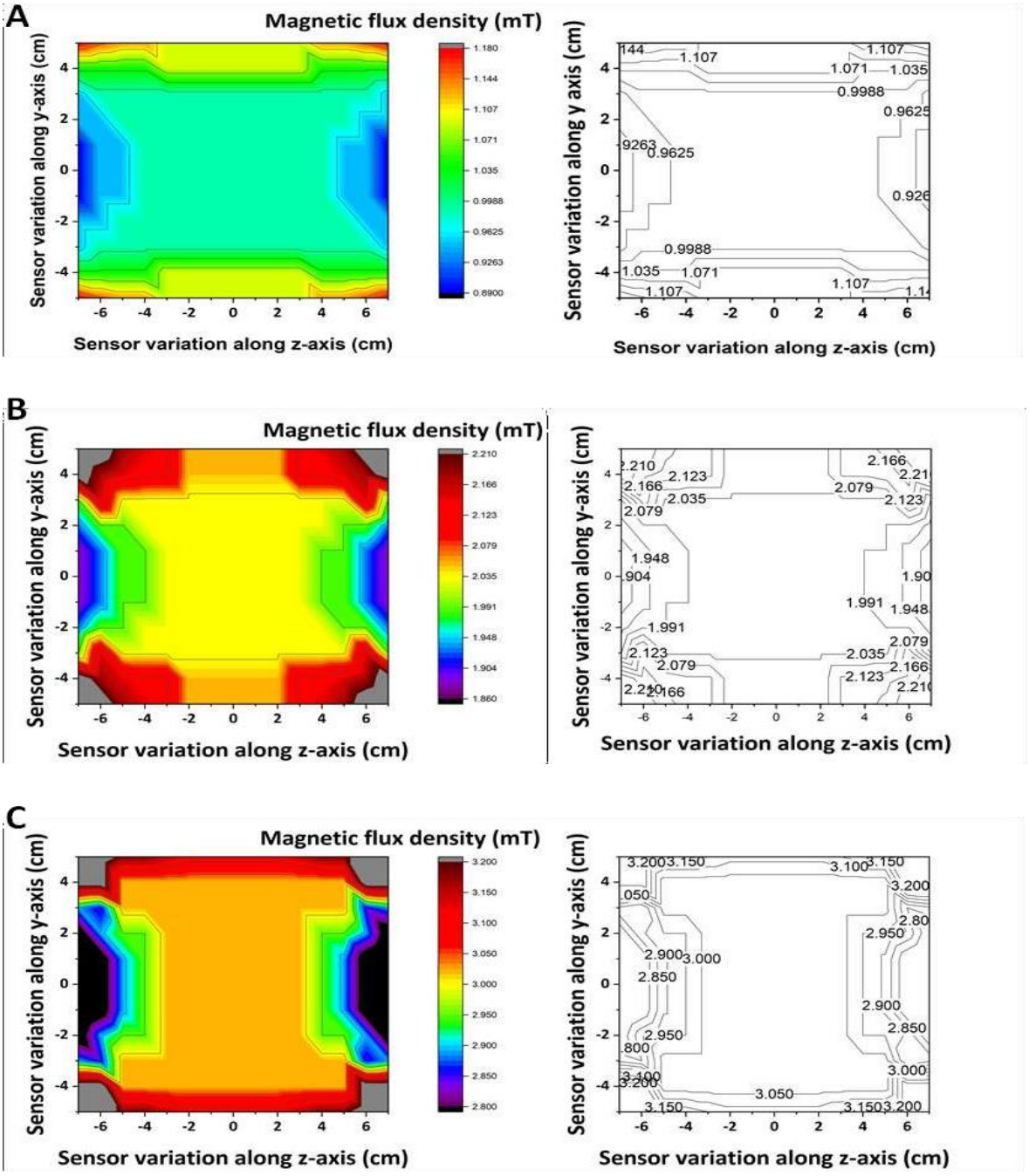

Figure 10. ELF-PEMF distributions between Helmholtz coils at different loading voltages. **(A)** Magnetic flux density vs sensor movement along the z-axis for a voltage and current range (V = 75 volts, I = 1.0 A), **(B)** Magnetic flux density vs sensor movement along the z-axis for a voltage and current range (V = 120 volts, I = 2.0 A), **(C)** Magnetic flux density vs sensor movement along the z-axis for a voltage and current range (V = 190 volts, I = 3.0 A).

Table 1. Theoretical Electrical parameters for Helmholtz coil system

No. of turns "N"	**Wire length (L_w) (m)**	**Resistance (Ω)**	**Current (A)**	**Voltage (V)**	**Power (W)**
540	898.668	23.3	1.00	75	75
540	898.668	23.3	2.00	132	264
540	898.668	23.3	3.00	189	567

Table 2. Electrical parameters obtained on Helmholtz coil prototype

No. of turns "N"	**Coil outer diameter (D) m**	**Wire diameter (d_w) m**	**Wire inductance (L_{wire}) H**	**Loop inductance (L_{loop}) H**	**Coil inductance (L_{coil}) H**	**Mutual inductance (M) H**	**Coupling factor (k)**
540	0.530	0.000914	2.55E+04	4.84E-09	4.53E-07	4.53E-07	1

Table 3. Electrical parameters obtained for generation and maintenance of uniform magnetic field

No. of turns "N"	**wire length (L_w) m**	**Measured resistance (Ω)**	**Max. current (A)**	**Max. voltage (V)**	**Max power (W)**	**Max magnetic field (mT)**
540	898.668	23.3	1.0	75	75	1.18
540	898.668	23.3	2.0	132	264	2.25
540	898.668	23.3	3.0	189	567	3.19

Table 4. Magnetic field homogeneity at the center of the Helmholtz coil system for $I = 1 - 3\ A$.

Area (cm^2) (30×35.5)	**Central field (mT)**	**Lowest field (mT)**	**Highest Field (mT)**	**(Field variation) (mT)**
I = 1 A	0.99	0.95	1.18	0.23

I = 2 A	2.0	1.94	2.25	0.31
I = 3 A	3.0	2.85	3.19	0.34

Table 5. Temperature variation in coils during the experimental duration

Current (A)	**Room temperature (T_R)**	**Initial temperature (T_1) ˚C**	**Final temperature (T_2) ˚C**	**Duration of exposure (min.)**
$I = 1\ A$	21.8	21.8	22.9	20
$I = 2\ A$	21.8	22.9	28.5	20
$I = 3\ A$	21.8	28.5	36.5	20